SIP30 Is Regulated by ERK in Peripheral Nerve Injury-induced Neuropathic Pain*[S]

Guangdun Peng[‡1], **Mei Han**[§1], **Yimin Du**[¶], **Anning Lin**[‖], **Lei Yu**[**], **Yuqiu Zhang**[§2], and **Naihe Jing**[‡3]

From the [‡]Laboratory of Molecular Cell Biology, Institute of Biochemistry and Cell Biology, Shanghai Institutes for Biological Sciences, Chinese Academy of Sciences, 320 Yue Yang Road, Shanghai 200031, China, [§]Institute of Neurobiology, Institutes of Brain Science and State Key Laboratory of Medical Neurobiology, Fudan University, Shanghai 200032, China, [¶]School of Life Sciences, Fudan University, Shanghai 200433, China, [‖]Ben May Department for Cancer Research, University of Chicago, Chicago, Illinois 60637, and [**]Department of Genetics and Center of Alcohol Studies, Rutgers University, Piscataway, New Jersey 08854

ERK plays an important role in chronic neuropathic pain. However, the underlying mechanism is largely unknown. Here we show that in chronic constriction injury-treated rat spinal cords, up-regulation of SIP30 (SNAP25-interacting protein 30), which is involved in the development and maintenance of chronic constriction injury-induced neuropathic pain, correlates with ERK activation and that the up-regulation of SIP30 is suppressed by intrathecal delivery of the MEK inhibitor U0126. In PC12 cells, up-regulation of SIP30 by nerve growth factor is also dependent on ERK activation. We found that there is an ERK-responsive region in the rat *sip30* promoter. Activation of ERK promotes the recruitment of the transcription factor cyclic AMP-response element-binding protein to the *sip30* gene promoter. Taken together, our results provide a potential downstream target of ERK activation-mediated neuropathic pain.

Neuropathic pain is a chronic painful condition due to nerve injury caused by trauma, disease, or surgical accidents. This kind of chronic pain brings severe distress, which disrupts the quality of life. There is a lack of effective treatment for neuropathic pain, and the underlying mechanism is poorly understood. Recently, attention has been focused on the central sensitization of spinal dorsal horn neurons, which are responsible for the modulation of neuropathic pain transmission. Central sensitization is a consequence of increased neuron excitability (1, 2). It has been shown that MAPKs[4] play a critical role in this sensitization and are responsible for the transduction of nociceptive signals (3). MAPKs are activated in the damaged neurons, and their inhibition can suppress or reverse neuropathic pain (4–9). In various pain models, ERK, a member of the MAPK family, is specifically activated in the superficial dorsal horn neurons by noxious but not innocuous stimulation. Inhibition of ERK activation alleviates pain hypersensitivity, indicating that ERK may play an important role in neuropathic pain (10–17).

ERK appears to regulate pain hypersensitivity in various aspects. It produces not only short term functional changes by post-translational processes, such as phosphorylation of membrane receptors and channels, but also long term adaptive alterations by changing gene expression (10, 12, 18, 19). Neuropathic pain is a chronic painful situation. It is believed that the long term gene expression regulated by ERK in the spinal cord plays a central role in the development of the disease (14). Thus, understanding of the molecular mechanism by which ERK regulates neuropathic pain is important to understand the pathology of central sensitization.

SIP30 (SNAP25-interacting protein 30) was first reported as a SNAP25-interacting protein of 30 kDa that functioned in vesicle trafficking (20). Through a differential screening of a rat brain cDNA library, we found that *sip30* was among the genes that were differentially expressed in the spinal cord CCI rats (21). We further showed that *sip30* mRNA and protein levels were up-regulated in the spinal cord of CCI-treated rats and that administration of SIP30 antisense oligonucleotides significantly suppressed CCI-induced pain hypersensitivity in both the onset and the continuous manifestation phases, suggesting that SIP30 may be functionally involved in the development and maintenance of chronic neuropathic pain (22). However, the mechanism underlying the regulation of *sip30* gene expression in this pathological process is unknown.

In this study, we show that SIP30 is regulated by ERK through the recruitment of cyclic AMP-response element-binding protein (CREB) to the promoter of the *sip30* gene, providing a novel mechanism by which ERK regulates CCI-induced neuropathic pain.

EXPERIMENTAL PROCEDURES

Animals and Drugs—Adult male Sprague-Dawley rats (200–280 g, from the Experimental Animal Center, Fudan University) were housed two per cage with free access to water and standard rat chow, with a 12:12-h day/night cycle and at a constant room temperature of 21 °C. All experimental protocols and animal handling procedures were consistent with the Chinese national standards for laboratory animal quality and the Chinese guidelines for the care and use of laboratory animals. All efforts were made to minimize the number of animals used.

A peripheral mononeuropathy was produced by loosely ligating the sciatic nerve according to a method described previously (23). Briefly, under pentobarbital sodium anesthesia (40 mg/kg, intraperitoneally), the right sciatic nerves were exposed at mid-thigh level by blunt dissection through the biceps femoris muscle. For CCI, four loosely constrictive ligatures (4-0 chromic gut suture) were tied around the nerve at a spacing of about 1 mm. The muscle and skin were closed in layers. For sham controls, the operation was performed to expose and mobilize the nerve, but the nerves were not ligated.

For intrathecal drug delivery, a polyethylene-10 catheter was implanted into the subarachnoid space of the spinal cord at the lumbar enlargement, and 10 μl of the MEK (ERK kinase) inhibitor U0126 (3 μg; Sigma, dissolved in 20% DMSO) was administered once daily for 4 days with the first application 4 h before CCI. DMSO (20%, Sigma) was injected as vehicle control.

Behavioral Testing—Behavioral testing was performed according to the method described previously (21). Briefly, the hind paw withdrawal threshold (PWT) was determined using a calibrated series of von Frey hairs (Stoelting Co., Wood Dale, IL) ranging from 1 to 26 g. Animals were placed individually into Plexiglas chambers with a customized platform that contains 1.5-mm diameter holes in a 5-mm grid of perpendicular rows throughout the entire area of the platform. The protocol used in this study was a variation of that described by Takaishi *et al.* (24). After acclimation to the test chambers, a series of nine calibrated von Frey hairs were applied to the central region of the plantar surface of one hind paw in ascending order (1, 1.4, 2, 4, 6, 8, 10, 15, and 26 g). A particular hair was applied until buckling of the hair occurred. This was maintained for ~2 s. The hair was applied only when the rat was stationary and standing on all four paws. A withdrawal response was considered valid only if the hind paw was completely removed from the customized platform. Each hair was applied five times at 5-s intervals. If withdrawal responses did not occur more than twice during five applications of a particular hair, the next ascending hair in the series was applied in a similar manner. Once the hind paw was withdrawn from a particular hair in three of the five consecutive applications, the rat was considered responsive to that hair. The PWT was defined as the lowest hair force in grams that produced at least three withdrawal responses in five tests. After the threshold was determined for one hind paw, the same testing procedure was repeated on the other hind paw at 5-min intervals.

Thermal hyperalgesia was assessed by measuring the latency of paw withdrawal (PWL) in response to a radiant heat source. Rats were placed individually into Plexiglas chambers on an elevated glass platform, under which a radiant heat source (model 336 combination unit, IITC/Life Science Instruments, Woodland Hill, CA) was applied to the glabrous surface of the paw through the glass plate. The heat source was turned off when the rat lifted the foot, allowing the measurement of time from onset of radiant heat application to withdrawal of the hind paw. This time was defined as the hind paw withdrawal latency. The heat was maintained at a constant intensity, which produced a stable PWL of ~10–12 s in the absence of arthritis. A 20-s cutoff was used to prevent tissue damage in the absence of a response. Both hind paws were tested for three trials at each time period with 10-min intervals between each trial. The average of the three trials was then determined.

Immunostaining—Immunostaining was performed as described previously (25). Briefly, CCI rats were deeply anesthetized with sodium pentobarbital and transcardially perfused with 50–100 ml of warm saline with heparin sodium, followed by 400 ml of 4% paraformaldehyde. Transverse spinal cord sections (30 μm) were cut and processed for immunostaining. The primary antibodies were rabbit anti-SIP30 (1:2000 (22)), mouse anti-phospho-ERK (1:500, Cell Signaling Technology), mouse anti-NeuN (neuronal marker, 1:500, Chemico), GFAP (astrocytic marker, 1:1000, Sigma), or OX-42 (microglial marker, 1:500, Serotec). Secondary antibodies were fluorescein isothiocyanate-conjugated donkey anti-rabbit/mouse IgG (1:500, Jackson ImmunoResearch) and rhodamine-conjugated donkey anti-rabbit IgG (1:500, Jackson ImmunoResearch), respectively. Normal mouse and rabbit IgGs (1:500, Zymed Laboratories Inc.) were used as the negative control. The images were captured with a Leica SP2 confocal laser-scanning microscope. The specificity of immunostaining was verified by omitting the primary antibodies (supplemental Fig. S1*C*). The specificity of the primary antibody was examined in HEK 293-T cells in which SIP30 is not internally expressed by Western blot and immunostaining (supplemental Fig. S1, *A* and *B*).

Cell Culture and Treatment—PC12 cells were cultured in Dulbecco's modified Eagle's medium containing 5% fetal bovine serum, 10% horse serum, 4 mM glutamine, 100 units/ml penicillin, and 0.2 mg/ml streptomycin under humidified conditions in 95% air and 5% CO_2 at 37 °C.

To examine SIP30 expression in NGF-induced PC12 cells, cells were plated onto 12-well 0.2% gelatin-coated plates for 24 h and serum-starved for at least 12 h before experiments. PC12 cells were pretreated with vehicle (0.2% DMSO) or MEK inhibitor U0126 (20 μM; Sigma, dissolved in 0.2% DMSO) for 1 h and then stimulated with NGF (50 ng/ml; Sigma) for the indicated times. Phosphorylated ERK and SIP30 protein levels were determined by immunoblotting, and *sip30* mRNA expression was examined by real time PCR.

For transfection, cells were plated onto gelatin-coated 6-well plates at 1×10^6 cells per well. The constitutively active form of MEK1 (CA-MEK1, S218E/S222E) or dominant negative MEK1 (DN-MEK1, K97M) was transfected into PC12 cells and maintained in low serum medium (1% fetal bovine serum/Dulbecco's modified Eagle's medium) in the presence of 50 ng/ml NGF for 24 h, then followed by immunoblotting or real time PCR analysis. Transient transfection was carried out using the
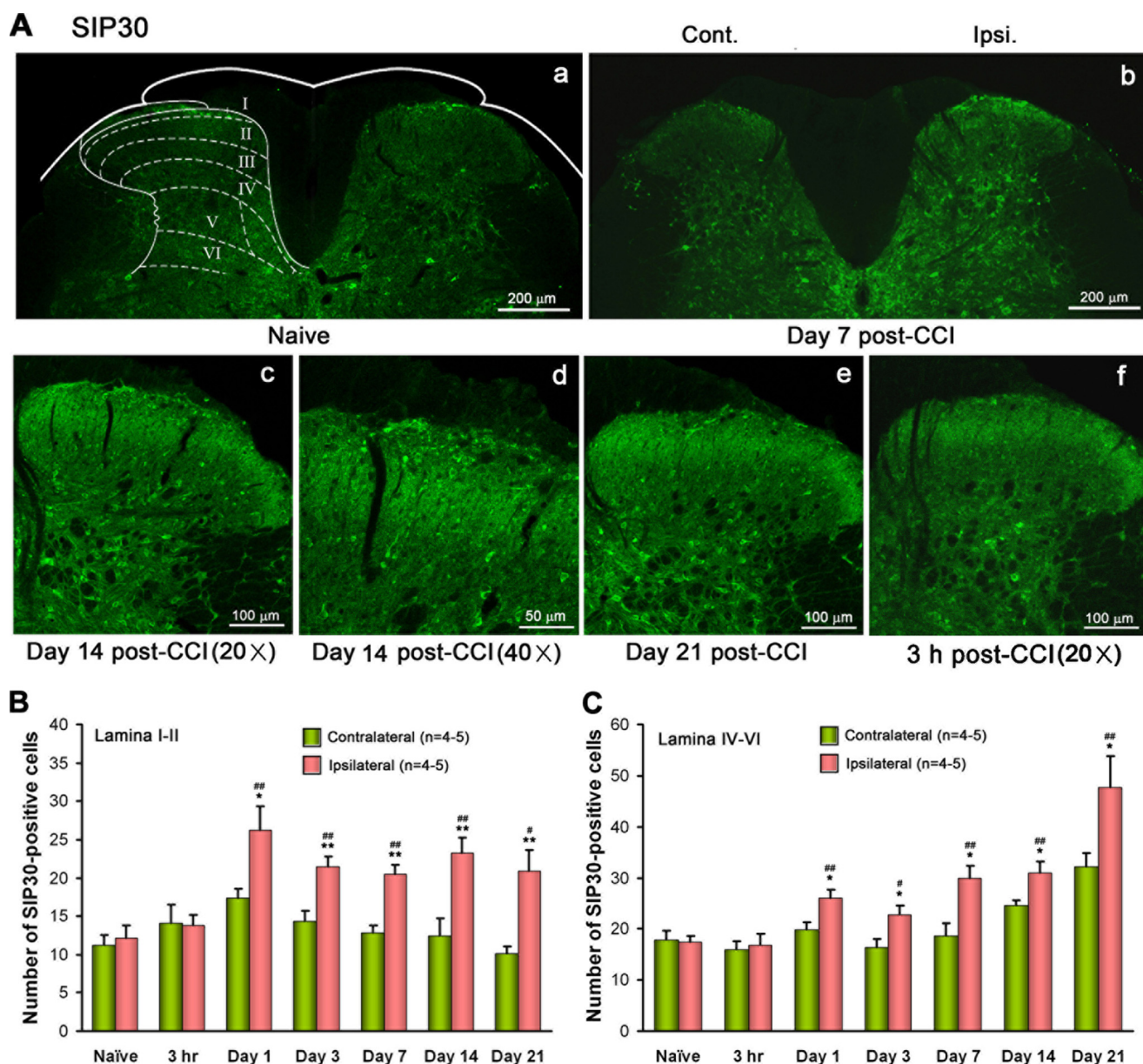
FIGURE 1. **SIP30 expression is up-regulated after CCI treatment in the spinal dorsal horn of CCI rats.** *A,* SIP30 immunoreactivity in the dorsal horn of the spinal cord is shown in naive (*panel a*), post-CCI surgery at 7 (*panel b*), 14 (*panels c* and *d*), and 21 days (*panel e*), and 3 h (*panel f*). Layers of I–VI in the rat spinal dorsal horn are indicated with *dashed lines*. *B* and *C,* time course of the mean SIP30-IR-positive neurons responding to CCI in the superficial layers (laminae I and II) (*B*) and deeper layers (laminae IV–VI) (*C*) were counted. The number of positive cells was evaluated in six sections through laminae IV–V segments for each animal. Four to five animals were used. *, $p < 0.05$; **, $p < 0.01$ *versus* ipsilateral (*Ipsi*); #, $p < 0.05$; ##, $p < 0.01$ *versus* naive. *Cont*, contralateral.

FuGENE HD transfection reagents (Roche Applied Science) according to the manufacturer's instructions.

Immunoblot Analysis—Western blot analysis was performed as described previously (26). Briefly, the cells or tissues were homogenized and harvested in 100 μl of lysis buffer containing 50 mM Tris-HCl (pH 8.0), 150 mM NaCl, 0.5% sodium deoxycholate, 0.1% SDS, 1% Nonidet P-40, 5 mM EDTA, 0.25 mM phenylmethanesulfonyl fluoride, and a mixture of protease inhibitors. The lysates were subjected to immunoblotting with the following primary antibodies: anti-phospho-ERK1/2 (1:2000, Cell Signaling Technology), anti-ERK (1:1000, Santa Cruz Biotechnology), and anti-SIP30 (22). For each blot, either the mouse monoclonal anti-α-tubulin (1:10,000, Sigma) or the anti-β-actin (1:7000, Sigma) was applied to serve as an internal

control. The autoradiography of x-ray films and the band intensity were processed using National Institutes of Health ImageJ software.

Real Time PCR—For reverse transcription, total RNA was extracted from PC12 cells by TRIzol (Invitrogen). Three micrograms of RNA was used as the template for first strand cDNA synthesis. Real time PCR was performed using an Eppendorf Realplex Cycler, as described previously (22). Briefly, the program was run in a final reaction volume of 20 μl containing the following reagents: 5.5 μl of PCR-grade water, 10 μl of 2× *Taq* mixture (Sigma), 0.5 μl of EvaGreen, 3 μl of cDNA template, and 0.5 μl of forward and reverse primer (20 μM). The amplification protocol included 3 min at 95 °C, followed by 40 cycles of 10 s of denaturation at 95 °C, 15 s of annealing at 58 °C, and 20-s
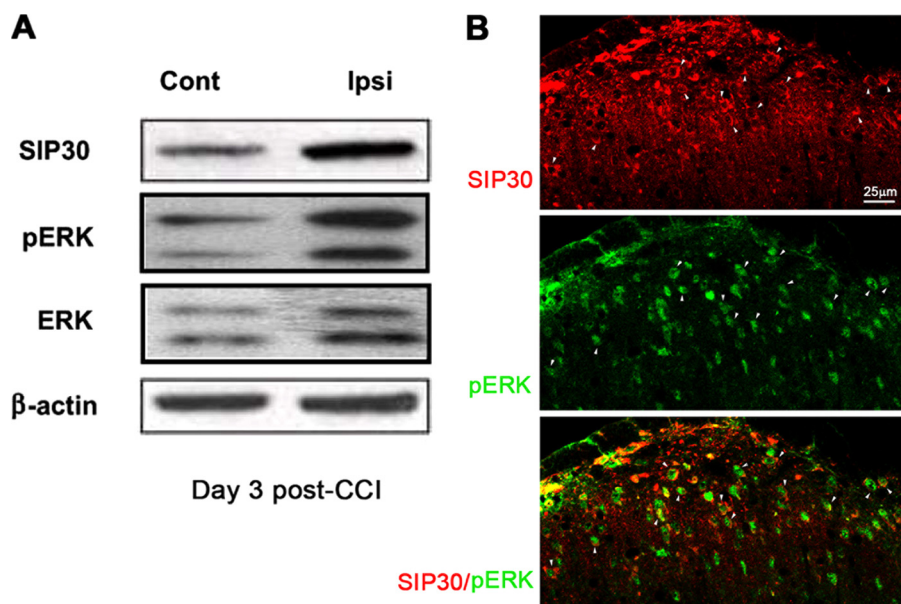
FIGURE 2. **SIP30 up-regulation correlates with ERK activation in the spinal dorsal horn of CCI rats.** *A,* spinal cords from rats 3 days post-CCI were subjected to immunoblotting. SIP30 and pERK expressions were examined. *Cont,* contralateral; *Ipsi,* ipsilateral. *B,* double immunostaining of activated ERK (*pERK, green*) and SIP30 (*red*) in the superficial layers of spinal dorsal horn in CCI rats indicated a co-localization of pERK and SIP30. *Arrowheads* indicate double-labeled cells.

extension at 72 °C. Each sample was run at least in triplicate, and C_t values were averaged from each reaction and then normalized to the *gapdh* value. The primers are listed in supplemental Table 1.

Construction of sip30 Promoter Luciferase Reporter—The 2.4-kb rat SIP30-Luc plasmid (5′*UTR-sip30-luc*) was generated by PCR amplification of the region upstream of the *sip30* translational start site, using the rat genomic DNA as a template. The region was then cloned into a pGL3 basic vector (Promega). Sequence fidelity was verified by sequencing analysis.

Luciferase Reporter Assay—Luciferase assay was performed as described previously (25). Briefly, PC12 cells were plated in a 24-well plate 1 day prior to transfection. Each well was transfected with a mixture of 0.8 μg of DNA, containing 0.1 μg of the reporter plasmid and 0.02 μg of pRL-TK (internal control) for 24 h. To detect luciferase activity, 100 μl of passive lysis buffer was added to each well for 1 h. The expression of luciferase and *Renilla* was determined using the Dual-Luciferase Reporter Assay kit (Promega) according to the manufacturer's instructions. Values were normalized to *Renilla* and plotted as a percentage relative to transfection with pcDNA3.

RNA Interference—Silencing of *creb* or *elk* was achieved by transfection of siRNAs targeting rat *creb* mRNA or *elk* mRNA, respectively. Two different *creb* siRNAs were introduced, corresponding to different regions of *creb* as follows: siCREB-1 (5′-GCACUUAAGGACCUUUACUtt-3′) and siCREB-2 (5′-GGAGUCUGUGGAUAGUGUAtt-3′). The siRNA duplexes for *elk* were siElk-1 (5′-GGTGAGCGGCCAGAAGTTT-3′) and siElk-2 (5′-CCTCTATTCTACCTTCACAAT-3). Scrambled RNA against *Thermotoga maritima* (5′-CUCCGAACGU-GUCACGUtt-3′) was used as a control. All siRNA duplexes were chemically synthesized by Shanghai GeneChem Co. Ltd. PC12 cells were plated in 12-well plates and transfected for 24 h with 50 nM siRNA or co-transfected with reporter plasmids

using Lipofectamine 2000 (Invitrogen) for 24 h. The cells were harvested for real time PCR analysis or assessment of luciferase activity.

Chromatin Immunoprecipitation (ChIP)—ChIP assay was performed according to the method described by Impey *et al.* (27). Briefly, PC12 cells were serum-starved for 12–16 h and stimulated with or without NGF for 1 h. Cells were fixed for 10 min with 1% formaldehyde at room temperature, and the cross-linking was stopped by the addition of 0.125 M glycine. Cells were washed and harvested with ice-cold phosphate-buffered saline and sonicated by a Bioruptor (Diagenode). Supernatants were transferred to fresh tubes and precleared with protein A-Sepharose. Immunoprecipitation was performed overnight at 4 °C with 10 μg of anti-CREB antibody (Millipore). Control groups were incubated with normal rabbit IgG. Immune complexes were captured with 30 μl of 50% protein A-agarose slurry (Santa Cruz Biotechnology) for 3 h at 4 °C. CREB-DNA complexes were then washed and eluted for reverse cross-linking. DNA fragments were purified by ethanol precipitation and quantified by real time PCR. Primers for ChIP assay are listed in supplemental Table 2.

Data Analysis—Total and phosphorylated ERK and SIP30 levels were quantified by scanning immunoblots with an HP2840 scanner. Data were calculated as the ratio of arbitrary densitometric units of phosphorylated ERK and SIP30 normalized to values obtained for total ERK or α-tubulin immunoreactive bands from the same immunoblots. The experiments were repeated at least three times. For the quantification of immunoreactive signals, six nonadjacent sections (30 μm) through the spinal laminae IV–V were randomly selected. The numbers of SIP30-labeled cells were counted in laminae I and II and laminae IV–VI under ×20 magnification, using a computerized image analysis system (Leica Qwin 500, Germany). Spinal regions were defined according to Molander *et al.* (28). Four to five rats were included in each group for quantification of immunohistochemistry results. All data are presented as mean ± S.D. or S.E. Parametric statistical analysis was performed using Student's *t* test (to compare two treatment groups) or a randomized one-way analysis of variance followed by Dunnett's test (for multiple group comparisons) to determine which groups were significantly different. Mean values were considered different if $p < 0.05$ (*, for $p < 0.05$; **, for $p < 0.01$).

RESULTS

Up-regulation of SIP30 Expression Correlates with Activation of ERK in the Spinal Dorsal Horn of CCI Rats—CCI causes persistent pain hypersensitivity (23, 29). Previously, we found that
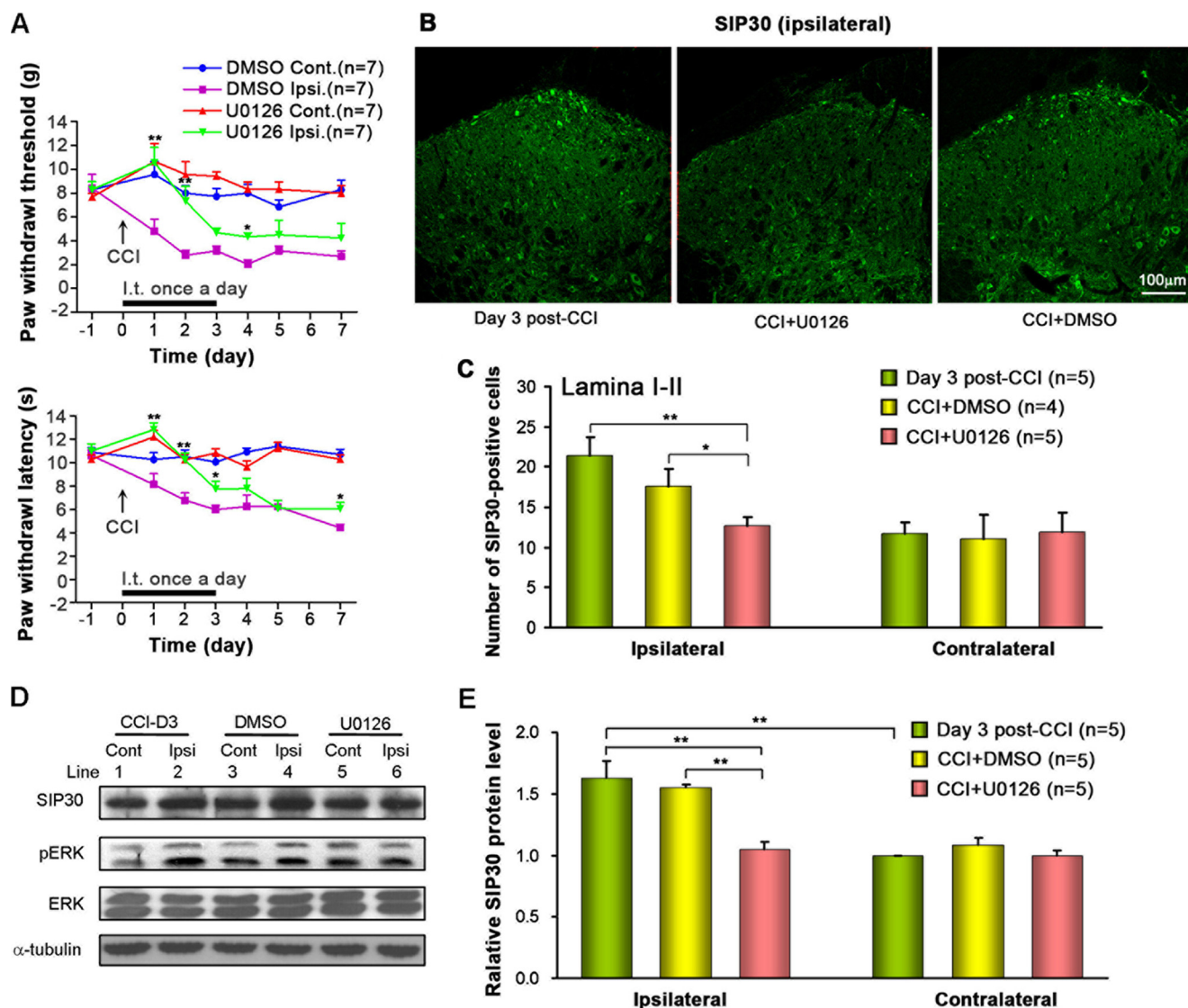
FIGURE 3. **Blockade of ERK activation attenuates CCI-induced behavioral hypersensitivity and SIP30 up-regulation in the spinal dorsal horn.** *A,* PWT to mechanical stimulus and PWL to thermal stimulus of the hind paws were analyzed. MEK inhibitor U0126 was intrathecally injected once a day for 4 days with the first application at 4 h before CCI, and vehicle of DMSO was used as the control. *Cont,* contralateral; *Ipsi,* ipsilateral. *B* and *C,* immunostaining of SIP30 after 3 days of CCI treatment with U0126 or vehicle DMSO injection was performed. Immunoreactive positive cells in laminae I and II of both sides were calculated. *D* and *E,* spinal cords of CCI rats injected with U0126 or vehicle DMSO were subjected to immunoblotting analysis. SIP30 level was semi-quantified by ImageJ software (National Institutes of Health), $n = 5$; *, $p < 0.05$; **, $p < 0.01$.

SIP30 is functionally involved in CCI-induced neuropathic pain (22). To understand how SIP30 expression is regulated in neuropathic pain, we examined spinal cord SIP30 expression in response to CCI by immunostaining. Prior to CCI treatment, SIP30-positive cells were mainly detected in laminae I and II and IV–VI of the dorsal horn where sensation fibers project. After unilateral CCI treatment, SIP30-positive cells increased significantly both in laminae I and II and IV–VI neurons of the ipsilateral spinal cord but not in the contralateral side (Fig. 1*A*). This increase occurred as early as the 1st day after CCI treatment and was sustained up to 3 weeks (Fig. 1, *A–C*). There are significant differences in SIP30-positive cells between ipsilateral sides and contralateral sides on both superficial layer (laminae I and II) and deep layer (laminae IV–VI) in the dorsal horn neurons of CCI rats (Fig. 1, *B* and *C*). Double immunofluorescence showed that almost all the SIP30-positive cells on the

spinal cord were neurons, because they co-expressed the neuronal marker NeuN (supplemental Fig. S2*A*).

Consistent with these findings, immunoblotting analysis revealed that although SIP30 protein was detectable at the contralateral side of spinal cord, its expression level was significantly up-regulated at the ipsilateral side upon CCI treatment. Interestingly, ERK phosphorylation was also significantly increased at the ipsilateral side in comparison with the contralateral side of spinal cord (Fig. 2*A*). In the contralateral spinal cord, phosphorylated ERK and SIP30 protein expression levels were not affected by CCI. Furthermore, double immunostaining revealed that CCI-induced phosphorylated ERK was co-localized with SIP30 in the same dorsal horn neurons (Fig. 2*B* and supplemental Fig. S2*B*). The parallel increase of SIP30 protein expression and ERK phosphorylation in the same spinal dorsal horn neurons suggests that activation of ERK may be
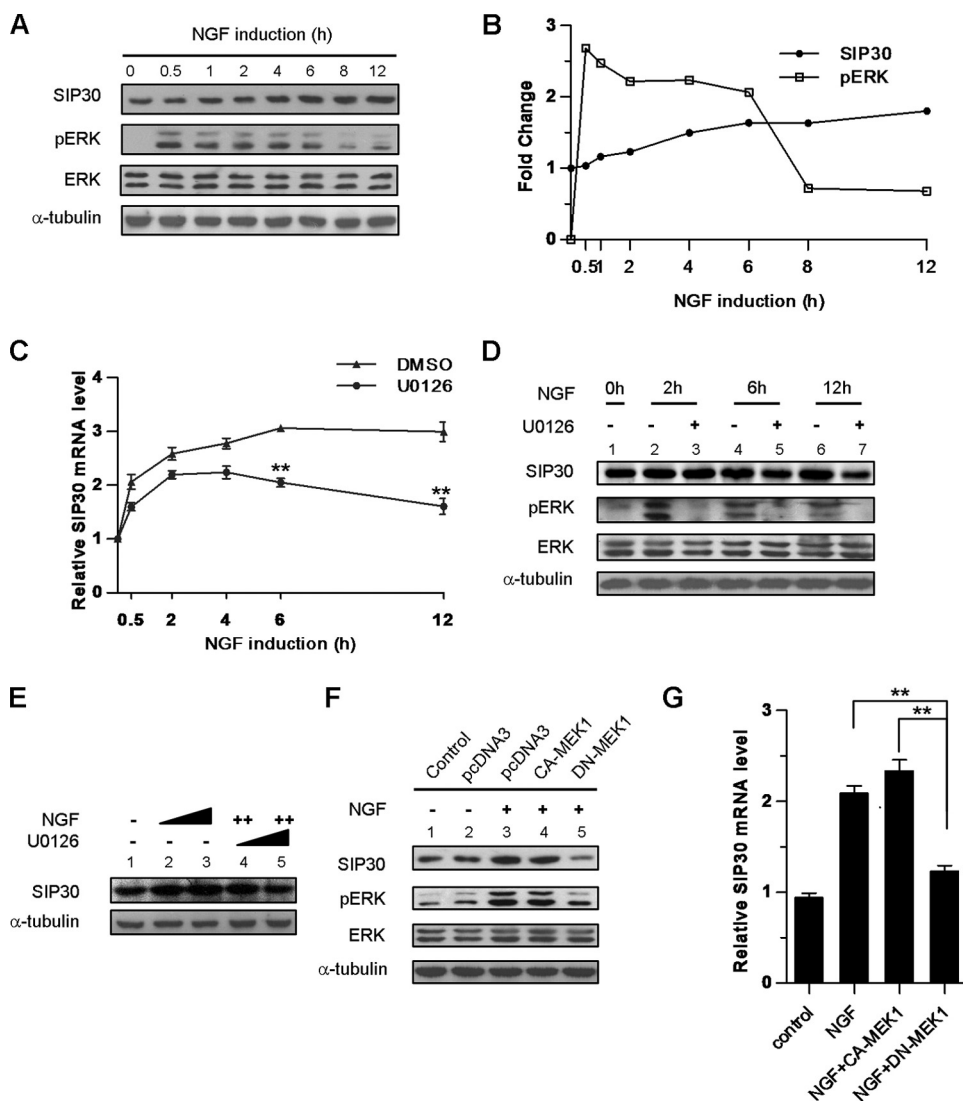
FIGURE 4. **NGF-induced up-regulation of SIP30 in PC12 cells is blocked by inhibition of ERK activation.** *A,* time course of SIP30 and pERK expression profile on stimulation with 50 ng/ml NGF for various times. *B,* fold change of SIP30 protein level was quantified by ImageJ software (National Institutes of Health). Normalized phosphorylated ERK (*pERK*) and SIP30 are shown on the *y* axis. *C* and *D,* PC12 cells were pretreated with U0126 (10 μM, 1 h) or vehicle DMSO, followed by stimulation with NGF (50 ng/ml) for various times. *sip30* mRNA change was analyzed by real time PCR, and SIP30 protein variation and ERK activation were analyzed by immunoblotting with anti-SIP30 and anti-pERK antibodies. *E,* PC12 cells were treated with increasing amounts of NGF (50 and 100 ng/ml) for 12 h or pretreated with increasing amounts of U0126 (10 and 20 μM) for 1 h and then stimulated with NGF (100 ng/ml) for an additional 12 h. SIP30 protein levels were checked by immunoblotting. *F* and *G,* PC12 cells were transfected with the constitutively activated MEK (*CA-MEK1*) or dominant negative MEK (*DN-MEK1*) and maintained in 1% fetal bovine serum/Dulbecco's modified Eagle's medium for 24 h in the presence of 50 ng/ml NGF. Protein and mRNA expressions of SIP30 were examined by immunoblotting and real time PCR, respectively **, $p < 0.01$.

in the ipsilateral hind paw for several days. U0126, however, produced no significant change on the PWT to von Frey hairs and PWL to thermal stimulation of the contralateral hind paw (Fig. 3*A*), suggesting that ERK may play a critical role in CCI-induced neuropathic pain, but it does not interfere with the normal pain sensation (30, 31).

To examine SIP30 expression after U0126 treatment, immunostaining and Western blot analysis were performed. The MEK inhibitor significantly suppressed CCI-induced increases in SIP30-positive neurons in the laminae I and II when compared with normal CCI or DMSO controls (Fig. 3, *B* and *C*). The suppression of SIP30 expression by U0126 was not obvious in the contralateral side of the spinal dorsal horn (Fig. 3*C*), suggesting that the interference of SIP30 expression caused by U0126 was constrained within the CCI-treated superficial dorsal horn of the spinal cord.

Under the same conditions, the ipsilateral side of the spinal cord displayed a significant increase in ERK phosphorylation 3 days after CCI (Fig. 3*D, pERK, lanes 1* and *2*), which was blocked by administering the MEK inhibitor U0126 (Fig. 3*D, pERK, lanes 5* and *6 versus lanes 1* and *2*). CCI also induced a robust up-regulation of SIP30 protein (Fig. 3*D, SIP30, lanes 1* and *2*), which was inhibited by the MEK inhibitor U0126 as well (Fig. 3*D, SIP30, lanes 5* and *6 versus lanes 1* and *2*; also see Fig. 3*E*). The intrathecal injection of the DMSO (control) had no detectable inhibitory effects (Fig. 3*D, SIP30, lanes 3* and *4 versus lanes 5* and *6*). On the contralateral side of the spinal cord, the MEK inhibitor U0126 exerted no detectable effects on SIP30 expression (Fig. 3*D, SIP30, lanes 1* and *3 versus lane 5*; Fig. 3*E*). Because the MEK inhibitor U0126 was delivered intrathecally, it should exert its effects on both ipsilateral and contralateral sides. Thus, U0126 inhibited CCI-induced up-regulation but not basal expression of SIP30. Taken together, these results show that CCI-induced up-regulation of SIP30 depends on ERK activation and that SIP30 may be a downstream target in the ERK signaling pathway that is involved in neuropathic pain.

involved in the up-regulation of SIP30 expression in CCI-induced pain induction and development.

Inhibition of ERK Activation Attenuates CCI-induced Behavioral Hypersensitivity and Reduces SIP30 Up-regulation in the Spinal Dorsal Horn—To explore whether ERK activation is involved in the SIP30 up-regulation in CCI-induced neuropathic pain, we applied the MEK-specific inhibitor U0126 to CCI rats, and we examined mechanical sensitivity by von Frey hair test and thermal sensitivity by Hargreave's test, as well as SIP30 expression in the spinal cord (Fig. 3). Intrathecal administration of this inhibitor significantly suppressed CCI-induced mechanical allodynia and thermal hyperalgesia

NGF-induced Up-regulation of SIP30 Is Blocked in PC12 Cells by Inhibiting ERK Activation—When grown in the presence of NGF, rat pheochromocytoma PC12 cells can differentiate into a sympathetic neuron-like phenotype (32). In many respects, the response of PC12 cells to NGF stimulation is similar to that of sympathetic neurons. It has been reported that NGF may be involved in chronic hyperalgesia (33–37), and NGF-induced pain hypersensitivity can be blocked by inhibiting ERK signaling (38). These findings prompted us to use NGF-induced PC12 cell differentiation as a model system to study the underlying mechanism between ERK activation and SIP30 up-regulation in CCI-induced neuropathic pain.

To determine the relationship between ERK activation and SIP30 expression, PC12 cells were first serum-starved and then stimulated with NGF. Immunoblotting analysis revealed that ERK was rapidly activated (Fig. 4, *A* and *B*). The activation lasted for several hours before gradually returning back to basal levels (Fig. 4, *A* and *B*) (39, 40). As seen in the rat spinal cord, PC12 cells expressed a basal level of SIP30 prior to NGF stimulation. The increased SIP30 expression occurred 4 h after NGF stimulation and lasted up to 12 h (Fig. 4, *A* and *B*). Thus, up-regulation of SIP30 by NGF correlates with ERK activation.

To determine whether ERK activation is required for NGF to induce SIP30 expression, PC12 cells were pretreated with or without U0126 for 1 h, followed by treatment with NGF. Real time PCR showed that NGF induced rapid and robust *sip30* mRNA expression, which was attenuated by the MEK inhibitor (Fig. 4*C*). Under the same conditions, U0126 also blocked NGF-induced ERK activation, as analyzed by immunoblotting (Fig. 4*D*). NGF-induced up-regulation of SIP30 occurred as early as 6 h and reached its maximum 12 h after NGF stimulation (Fig. 4*D*, *SIP30, lanes 1, 4,* and *6*). Interestingly, the MEK inhibitor effectively blocked NGF-induced up-regulation but not basal levels of SIP30 (Fig. 4*D*, *SIP30, lanes 4 versus 5* and *lanes 6 versus 7* compared with *lanes 1 versus 3, 5,* and *7*), similar to the CCI-induced up-regulation of SIP30 observed in rat spinal cord. Furthermore, SIP30 protein levels were up-regulated by NGF in a dose-dependent manner (Fig. 4*E, lanes 1–3*), and this up-regulation was inhibited by the MEK inhibitor U0126 (Fig. 4*E, lanes 3–5*). Overexpression of a dominant negative MEK1 construct (DN-MEK1) also inhibited NGF-induced ERK activation and up-regulation of SIP30 (Fig. 4*F, lanes 3 versus 5*). The constitutively active MEK1 construct (CA-MEK1) did not further enhance NGF-induced ERK activation or SIP30 expression, suggesting that endogenous MEK1 was sufficient to mediate NGF effects. Real time PCR showed that NGF significantly induced *sip30* mRNA expression, which was slightly enhanced by ectopic expression of CA-MEK1 and significantly suppressed by DN-MEK1 (Fig. 4*G*). Taken together, these results show that NGF up-regulates SIP30 expression through the MEK1-ERK pathway in PC12 cells, most likely at the level of gene transcription.

ERK Is Involved in the Regulation of the sip30 Promoter Activity—To determine how ERK regulates SIP30 expression, we performed an *in vitro* luciferase reporter assay. A 2.4-kb fragment of the 5′ upstream region of the rat *sip30* gene was subcloned into a luciferase reporter vector (Fig. 5*A, 5′UTR-sip30-luc*). After transfection into PC12 cells, this genomic
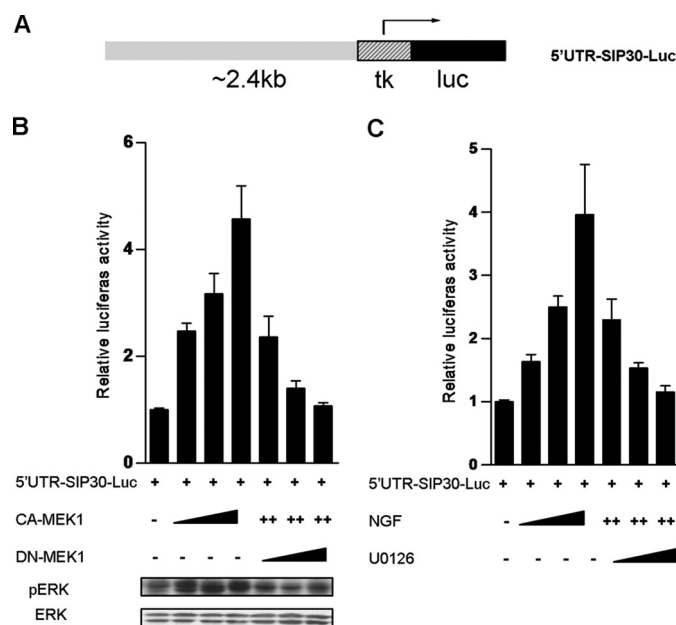

FIGURE 5. **ERK is involved in the regulation of *sip30* promoter activity.** *A,* rat *sip30* gene promoter-reporter construct. The *underlined* 2.4-kb fragment was cloned into pGL3-basic vector (*5′UTR-SIP30-Luc*) by KpnI and NheI double digestion and used to check reporter activity. *tk,* thymidine kinase. *B,* luciferase (*luc*) reporter assay was performed by transfection of 5′UTR-SIP30-Luc with increasing amounts of CA-MEK1 (0.1, 0.25, and 0.5 μg, respectively) or with increasing amounts of DN-MEK1 (0.1, 0.25, and 0.5 μg respectively, combined with 0.25 μg of CA-MEK1) for 24 h. ERK activity after transfection was checked by Western blot (*lower panel*). *C,* transfected PC12 cells were treated by varying the dose of NGF (50, 100, and 200 ng/ml) for 24 h or pretreated by U0126 (5, 10, and 20 μM, 1 h) followed by 100 ng/ml NGF stimulation for 24 h, and luciferase activity was examined.

sequence showed a strong luciferase activity (data not shown), indicating that this 2.4-kb UTR region has promoter activity. The promoter activity of the reporter gene was stimulated by co-transfection with CA-MEK1 in a dose-dependent manner (Fig. 5*B*). The stimulation by CA-MEK1 was blocked by co-transfection with DN-MEK1 (Fig. 5*B*). In agreement with these findings, NGF stimulated *sip30* promoter activity in a dose-dependent manner and pretreatment with the MEK1 inhibitor U0126 significantly attenuated NGF-induced *sip30* promoter activity (Fig. 5*C*). Together, these results show that the MEK1-ERK pathway may regulate the promoter activity of the *sip30* gene.

ERK Regulates sip30 Expression through CREB, Which Binds to the sip30 Promoter to Stimulate Its Expression—ERK activates a variety of transcription factors that in turn regulate the expression of many target genes (41). We first checked whether Ets-like transcription factor-1 (Elk-1) was involved in the regulation of *sip30* expression. Two siRNA duplexes targeting *elk-1* (siElk-1 and siElk-2) were synthesized and transfected into NGF-stimulated PC12 cells. The Elk expression can be significantly reduced by siElk-2 (Fig. 6*B*). However, NGF-stimulated *sip30* up-regulation was not affected by Elk siRNA transfection, indicating that Elk has a marginal effect for ERK-mediated *sip30* up-regulation (Fig. 6*C*).

The nuclear CREB is another key downstream transcription factor of ERK signaling. It is known that in NGF-stimulated PC12 cells, CREB is phosphorylated by ERK and in turn regulates the expression of many NGF target genes (42, 43). We
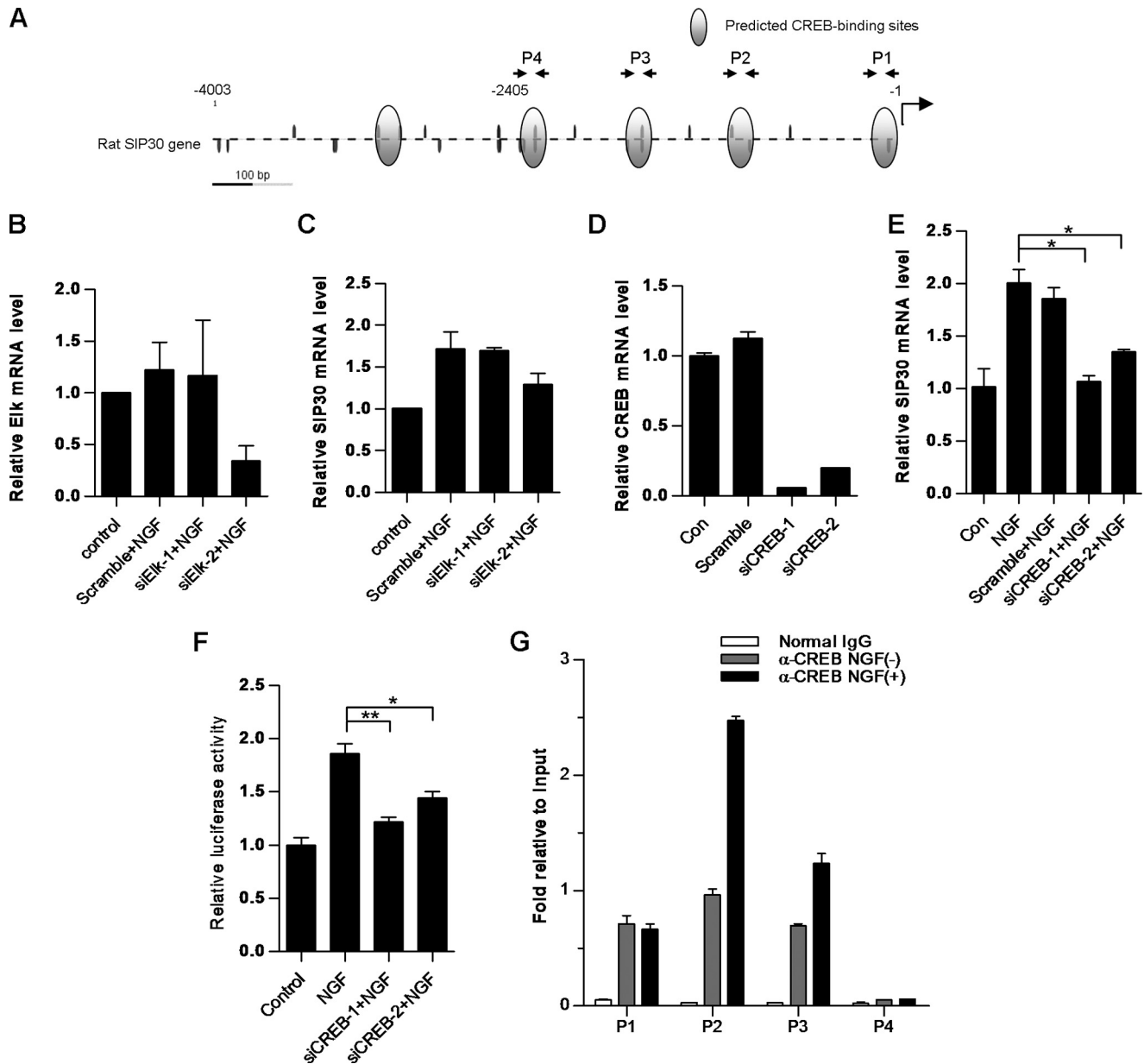
FIGURE 6. **ERK mediates NGF-induced SIP30 up-regulation via CREB binding in the *sip30* promoter.** *A,* diagram of predicted conserved CREB-binding sites in SIP30 5′UTR (∼4 kb). *B,* two Elk siRNAs duplexes (50 nM) were transfected into NGF-treated PC12 cells. The knockdown effect of siRNAs (*B*) and SIP30 expression (*C*) was checked by real time PCR. *D,* two synthesized CREB siRNAs (50 nM) were both transfected into PC12 cells for 24 h. CREB expression was checked by real time PCR. *Con,* control. *E,* CREB siRNAs were transfected into PC12 cells in the presence of NGF stimulation, and SIP30 expression level was examined by real time PCR. *F,* PC12 cells were transfected with 5′UTR-SIP30-Luc and siCREB in the presence of NGF (50 ng/ml) for 24 h. Promoter luciferase activity was examined. *G,* ChIP was performed using CREB antibody. PC12 cells were treated with or without NGF for 1 h and then subjected to ChIP assay. The fold increase of immunoprecipitated *sip30* promoter regions obtained by anti-CREB *versus* normal IgG was measured by real time PCR. Values based on real time PCR were normalized to input. Four primers were used to run real time PCR. The position of the primers is indicated in *A* and is shown in supplemental Table 2. *, $p < 0.05$; **, $p < 0.01$.

observed a correlation between ERK activation and CREB phosphorylation during NGF-induced PC12 cell differentiation (supplemental Fig. S3). Using a theoretical transcription factor analysis program (Genomatix MatInspector), we identified four conserved CREB-binding sites, named P1, P2, P3, and P4, in the above 2.4-kb upstream region of the *sip30* gene across different species (Fig. 6*A*), suggesting that CREB may be involved in *sip30* expression.

The above observation prompted us to test whether CREB is one of the downstream targets of the NGF-activated ERK pathway that up-regulate *sip30* expression. Indeed, NGF-induced

elevation of *sip30* mRNA was inhibited by two different siRNAs for *creb* (Fig. 6*E*), which significantly reduced *creb* expression but not the scrambled siRNA in PC-12 cells (Fig. 6*D*). Additionally, NGF-stimulated *sip30* promoter activity was significantly inhibited by siCREBs (Fig. 6*F*). Furthermore, ChIP assay showed that CREB was only recruited to the conserved CREB sites P1, P2, and P3 but not the P4 site in the *sip30* promoter, as determined by quantitative PCR (Fig. 6*G*). NGF treatment promoted the recruitment of CREB to P2 and P3 (especially P2) in the *sip30* promoter (Fig. 6*G*), suggesting that NGF-induced *sip30* expression was mainly dependent on the recruitment of
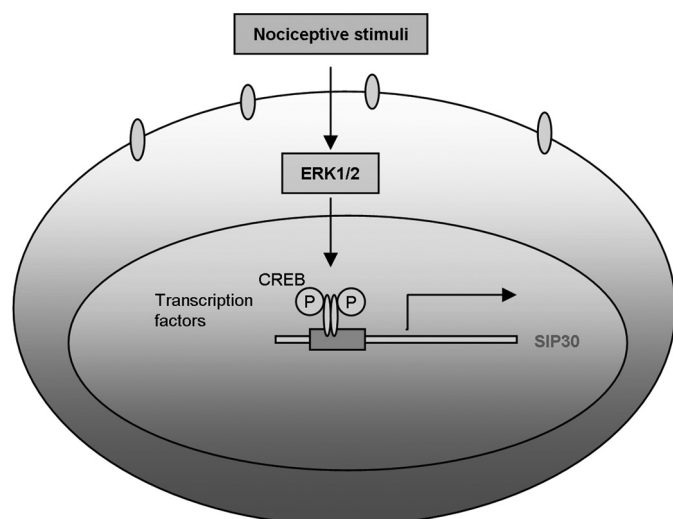
FIGURE 7. Putative model to elucidate the relationship between ERK and SIP30 in neuropathic pain. See "Discussion" for the details.

CREB to P2 and P3 in the *sip30* promoter. Taken together, these results indicate that ERK signaling regulates NGF-up-regulated *sip30* expression by promoting the recruitment of CREB to the *sip30* gene promoter.

DISCUSSION

SIP30 is involved in neuropathic pain development and maintenance, but the precise regulation of SIP30 expression remains elusive. In this study, we show that CCI-induced up-regulation of SIP30 correlates with ERK activation in the dorsal spinal cord neurons (Figs. 1 and 2). Furthermore, SIP30 up-regulation was partially suppressed in the CCI-operated side of the rat spinal cord when ERK activation was inhibited by intrathecal delivery of the MEK inhibitor U0126 (Fig. 3). In NGF-induced PC12 cells, *sip30* was regulated by ERK activation in a transcription-dependent manner, and NGF stimulated the recruitment of the transcription factor CREB, a downstream target of ERK, to the *sip30* gene promoter (Figs. 4–6). These observations prompted us to hypothesize that, in neuropathic pain, extracellular nociceptive stimulus activates ERK, which in turn phosphorylates downstream transcription factors such as CREB (17, 44–47) and promotes the recruitment of CREB to the *sip30* promoter to up-regulate its expression (Fig. 7).

A common and severely debilitating symptom of neuropathic pain is hyperalgesia, which is refractory or resistant to conventional analgesics. The failure of analgesics may stem from central sensitization caused by persistent C/Aβ fiber input to the spinal cord and subsequently long term changes in dorsal horn neurons (48). Although it is well known that ERK activation contributes to pain central sensitization, it is problematic for anti-pain drugs to target ERK, considering the extensive role and multiple effectors of ERK in responding to various extracellular stimulus (49, 50). We found that intrathecal injection of the MEK inhibitor U0126 not only delayed the development of mechanical allodynia and thermal hyperalgesia (Fig. 3*A*) but also reversed the establishment of pain abnormality (data not shown), suggesting the involvement of ERK and its regulation of gene expression in CCI nerve injury. We found

that SIP30 was up-regulated during both the development and the maintenance phases of CCI and that knocking down SIP30 has similar effect to ERK inhibition on neuropathic pain behavior (Fig. 1*B*) (22). Although basal expression of SIP30 was not affected by inhibition of the ERK pathway, the stimulus-induced SIP30 expression was regulated by ERK in both *in vivo* and *in vitro* models (Figs. 3 and 4). Thus, SIP30 may be involved in ERK-dependent long term pain modulation. These findings might provide a potential therapeutic strategy to develop drugs that can interfere with SIP30 expression without affecting ERK activity for the prevention and treatment of chronic neuropathic pain.

CREB is known to play an important role in transducing pain signals (17, 45, 51–54). CREB can be phosphorylated by various extracellular stimuli, and ERK then inducibly binds to the promoters of many genes to regulate their transcription (55). In the NGF-stimulated cell model, we found that CREB mediated ERK-regulated *sip30* expression, and NGF promoted the recruitment of CREB to the *sip30* promoter (Fig. 6). Based on the information gathered from mapping of the CREB binding regions over human chromosome 22, there are several soluble NSF attachment protein receptor family members, such as SYN3 and SNAP29, to be downstream targets of CREB (56). Thus, it is possible that *sip30* may function as a CREB target in CCI rats.

In learning and memory behaviors, the importance of ERK in long term potentiation (LTP) is well established (57). Pain shares many similar mechanisms with learning and memory (1). Spinal LTP can also be induced in pain pathways and contributes to hyperalgesia caused by inflammation, trauma, or neuropathy (58). Although the ERK pathway is necessary for the induction and maintenance of pain LTP (59), the precise role of ERK remains elusive. SIP30 was first characterized as a protein that interacts with SNAP25 (20). Considering the critical role of SNAP25 in exocytosis and regulating neural plasticity (60–62), SIP30 is likely involved in mediating long term pain plasticity and LTP. This hypothesis is in agreement with a recent paper in which SIP30 was identified as a long term memory consolidation associated gene in opiate addiction (63). Furthermore, SIP30 would be probably located in spinal excitatory interneurons to enhance neuron excitability, as hippocampal GABAergic inhibitory synapses lack SNAP-25 (64, 65). Therefore, our work suggests that ERK may mediate pain LTP through the regulation of SIP30 expression.

REFERENCES

1. Ji, R. R., Kohno, T., Moore, K. A., and Woolf, C. J. (2003) *Trends Neurosci.* **26,** 696–705
2. Campbell, J. N., and Meyer, R. A. (2006) *Neuron* **52,** 77–92
3. Lim, G., Sung, B., Ji, R. R., and Mao, J. (2003) *Pain* **105,** 275–283
4. Zhuang, Z. Y., Gerner, P., Woolf, C. J., and Ji, R. R. (2005) *Pain* **114,** 149–159
5. Obata, K., and Noguchi, K. (2004) *Life Sci.* **74,** 2643–2653
6. Obata, K., Katsura, H., Mizushima, T., Sakurai, J., Kobayashi, K., Yamanaka, H., Dai, Y., Fukuoka, T., and Noguchi, K. (2007) *J. Neurochem.* **102,** 1569–1584
7. Ji, R. R., Kawasaki, Y., Zhuang, Z. Y., Wen, Y. R., and Zhang, Y. Q. (2007) *Handb. Exp. Pharmacol.* **177,** 359–389
8. Zhuang, Z. Y., Wen, Y. R., Zhang, D. R., Borsello, T., Bonny, C., Strichartz, G. R., Decosterd, I., and Ji, R. R. (2006) *J. Neurosci.* **26,** 3551–3560

9. Ji, R. R., Kawasaki, Y., Zhuang, Z. Y., Wen, Y. R., and Decosterd, I. (2006) *Neuron Glia Biol.* **2,** 259–269

10. Dai, Y., Iwata, K., Fukuoka, T., Kondo, E., Tokunaga, A., Yamanaka, H., Tachibana, T., Liu, Y., and Noguchi, K. (2002) *J. Neurosci.* **22,** 7737–7745

11. Ji, R. R., Samad, T. A., Jin, S. X., Schmoll, R., and Woolf, C. J. (2002) *Neuron* **36,** 57–68

12. Ji, R. R., Befort, K., Brenner, G. J., and Woolf, C. J. (2002) *J. Neurosci.* **22,** 478–485

13. Galan, A., Lopez-Garcia, J. A., Cervero, F., and Laird, J. M. (2002) *Neurosci. Lett.* **322,** 37–40

14. Ciruela, A., Dixon, A. K., Bramwell, S., Gonzalez, M. I., Pinnock, R. D., and Lee, K. (2003) *Br. J. Pharmacol.* **138,** 751–756

15. Galan, A., Cervero, F., and Laird, J. M. (2003) *Brain Res. Mol. Brain Res.* **116,** 126–134

16. Tseng, T. J., Hsieh, Y. L., and Hsieh, S. T. (2007) *Exp. Neurol.* **206,** 17–23

17. Crown, E. D., Ye, Z., Johnson, K. M., Xu, G. Y., McAdoo, D. J., and Hulsebosch, C. E. (2006) *Exp. Neurol.* **199,** 397–407

18. Ji, R. R., Baba, H., Brenner, G. J., and Woolf, C. J. (1999) *Nat. Neurosci.* **2,** 1114–1119

19. Karim, F., Wang, C. C., and Gereau, R. W., 4th (2001) *J. Neurosci.* **21,** 3771–3779

20. Lee, H. K., Safieddine, S., Petralia, R. S., and Wenthold, R. J. (2002) *J. Neurochem.* **81,** 1338–1347

21. Wang, X., Zhang, Y., Kong, L., Xie, Z., Lin, Z., Guo, N., Strong, J. A., Meij, J. T., Zhao, Z., Jing, N., and Yu, L. (2005) *Eur. J. Neurosci.* **22,** 1090–1096

22. Zhang, Y. Q., Guo, N., Peng, G., Han, M., Raincrow, J., Chiu, C., Coolen, L. M., Wenthold, R. J., Zhao, Z. Q., Jing, N. H., and Yu, L. (2009) *Pain,*

23. Bennett, G. J., and Xie, Y. K. (1988) *Pain* **33,** 87–107

24. Takaishi, K., Eisele, J. H., Jr., and Carstens, E. (1996) *Pain* **66,** 297–306

25. Gao, X., Bian, W., Yang, J., Tang, K., Kitani, H., Atsumi, T., and Jing, N. (2001) *Biochem. Biophys. Res. Commun.* **284,** 1098–1103

26. Shen, C., Chen, Y., Liu, H., Zhang, K., Zhang, T., Lin, A., and Jing, N. (2008) *J. Biol. Chem.* **283,** 17721–17730

27. Impey, S., McCorkle, S. R., Cha-Molstad, H., Dwyer, J. M., Yochum, G. S., Boss, J. M., McWeeney, S., Dunn, J. J., Mandel, G., and Goodman, R. H. (2004) *Cell* **119,** 1041–1054

28. Molander, C., Xu, Q., and Grant, G. (1984) *J. Comp. Neurol.* **230,** 133–141

29. Moalem, G., Xu, K., and Yu, L. (2004) *Neuroscience* **129,** 767–777

30. Garry, E. M., Delaney, A., Blackburn-Munro, G., Dickinson, T., Moss, A., Nakalembe, I., Robertson, D. C., Rosie, R., Robberecht, P., Mitchell, R., and Fleetwood-Walker, S. M. (2005) *Mol. Cell. Neurosci.* **30,** 523–537

31. Obata, K., Yamanaka, H., Dai, Y., Mizushima, T., Fukuoka, T., Tokunaga, A., and Noguchi, K. (2004) *Eur. J. Neurosci.* **20,** 2881–2895

32. Greene, L. A., and Tischler, A. S. (1976) *Proc. Natl. Acad. Sci. U.S.A.* **73,** 2424–2428

33. McMahon, S. B. (1996) *Philos. Trans. R. Soc. Lond. B Biol. Sci.* **351,** 431–440

34. Herzberg, U., Eliav, E., Dorsey, J. M., Gracely, R. H., and Kopin, I. J. (1997) *Neuroreport* **8,** 1613–1618

35. Ro, L. S., Chen, S. T., Tang, L. M., and Jacobs, J. M. (1999) *Pain* **79,** 265–274

36. Hefti, F. F., Rosenthal, A., Walicke, P. A., Wyatt, S., Vergara, G., Shelton, D. L., and Davies, A. M. (2006) *Trends Pharmacol. Sci.* **27,** 85–91

37. Sah, D. W., Ossipo, M. H., and Porreca, F. (2003) *Nat. Rev. Drug Discov.* **2,** 460–472

38. Malik-Hall, M., Dina, O. A., and Levine, J. D. (2005) *Eur. J. Neurosci.* **21,** 3387–3394

39. Gómez, N., and Cohen, P. (1991) *Nature* **353,** 170–173

40. Santos, S. D., Verveer, P. J., and Bastiaens, P. I. (2007) *Nat. Cell Biol.* **9,** 324–330

41. Ji, R. R., Gereau, R. W., Malcangio, M., and Strichartz, G. R. (2009) *Brain Res. Rev.* **60,** 135–148

42. Riccio, A., Pierchala, B. A., Ciarallo, C. L., and Ginty, D. D. (1997) *Science* **277,** 1097–1100

43. Riccio, A., Ahn, S., Davenport, C. M., Blendy, J. A., and Ginty, D. D. (1999) *Science* **286,** 2358–2361

44. Yu, C. G., and Yezierski, R. P. (2005) *Brain Res. Mol. Brain Res.* **138,** 244–255

45. Song, X. S., Cao, J. L., Xu, Y. B., He, J. H., Zhang, L. C., and Zeng, Y. M. (2005) *Acta Pharmacol. Sin.* **26,** 789–798

46. Josiah, D. T., and Vincler, M. A. (2006) *Psychopharmacology* **188,** 152–161

47. Kawasaki, Y., Kohno, T., Zhuang, Z. Y., Brenner, G. J., Wang, H., Van Der Meer, C., Befort, K., Woolf, C. J., and Ji, R. R. (2004) *J. Neurosci.* **24,** 8310–8321

48. Basbaum, A. I., and Woolf, C. J. (1999) *Curr. Biol.* **9,** R429–R431

49. Ji, R. R. (2004) *Curr. Opin. Investig. Drugs* **5,** 71–75

50. Sebolt-Leopold, J. S., and Herrera, R. (2004) *Nat. Rev.* **4,** 937–947

51. Ji, R. R., and Rupp, F. (1997) *J. Neurosci.* **17,** 1776–1785

52. Hoeger-Bement, M. K., and Sluka, K. A. (2003) *J. Neurosci.* **23,** 5437–5445

53. Ma, W., and Quirion, R. (2001) *Pain* **93,** 295–301

54. Ma, W., Hatzis, C., and Eisenach, J. C. (2003) *Brain Res.* **988,** 97–104

55. Shaywitz, A. J., and Greenberg, M. E. (1999) *Annu. Rev. Biochem.* **68,** 821–861

56. Euskirchen, G., Royce, T. E., Bertone, P., Martone, R., Rinn, J. L., Nelson, F. K., Sayward, F., Luscombe, N. M., Miller, P., Gerstein, M., Weissman, S., and Snyder, M. (2004) *Mol. Cell. Biol.* **24,** 3804–3814

57. Sweatt, J. D. (1999) *Learn. Mem.* **6,** 399–416

58. Sandkühler, J. (2007) *Mol. Pain* **3,** 9

59. Xin, W. J., Gong, Q. J., Xu, J. T., Yang, H. W., Zang, Y., Zhang, T., Li, Y. Y., and Liu, X. G. (2006) *J. Neurosci. Res.* **84,** 934–943

60. Xu, N. J., Yu, Y. X., Zhu, J. M., Liu, H., Shen, L., Zeng, R., Zhang, X., and Pei, G. (2004) *J. Biol. Chem.* **279,** 40601–40608

61. Hou, Q. L., Gao, X., Lu, Q., Zhang, X. H., Tu, Y. Y., Jin, M. L., Zhao, G. P., Yu, L., Jing, N. H., and Li, B. M. (2006) *Biochem. Biophys. Res. Commun.* **347,** 955–962

62. Bark, C., Bellinger, F. P., Kaushal, A., Mathews, J. R., Partridge, L. D., and Wilson, M. C. (2004) *J. Neurosci.* **24,** 8796–8805

63. Marie-Claire, C., Courtin, C., Robert, A., Gidrol, X., Roques, B. P., and Noble, F. (2007) *Neuropharmacology* **52,** 430–435

64. Verderio, C., Pozzi, D., Pravettoni, E., Inverardi, F., Schenk, U., Coco, S., Proux-Gillardeaux, V., Galli, T., Rossetto, O., Frassoni, C., and Matteoli, M. (2004) *Neuron* **41,** 599–610

65. Frassoni, C., Inverardi, F., Coco, S., Ortino, B., Grumelli, C., Pozzi, D., Verderio, C., and Matteoli, M. (2005) *Neuroscience* **131,** 813–823